Computer-Aided Design 43 (2011) 1011–1017

Contents lists available at ScienceDirect

Computer-Aided Design

journal homepage: www.elsevier.com/locate/cad

Curvature continuous offset approximation based on circle approximation using quadratic Bézier biarcs

Young Joon Ahn [a,*], Christoph Hoffmann [b], Yeon Soo Kim [c]

[a] Department of Mathematics Education, Chosun University, Gwangju, 501–759, South Korea
[b] Department of Computer Science, Purdue University, West Lafayette, IN 47907, USA
[c] Department of Mathematics, Ajou University, Suwon, 442–749, South Korea

ARTICLE INFO

Article history:
Received 6 June 2010
Accepted 12 April 2011

Keywords:
Offset curve
Hausdorff distance
Convolution curve
Curvature continuous interpolation
Circle approximation
Quadratic Bézier biarcs

ABSTRACT

We present a method for G^2 end-point interpolation of offset curves using rational Bézier curves. The method is based on a G^2 end-point interpolation of circular arcs using quadratic Bézier biarcs. We also prove the invariance of the Hausdorff distance between two compatible curves under convolution. Using this result, we obtain the exact Hausdorff distance between an offset curve and its approximation by our method. We present the approximation algorithm and give numerical examples.

1. Introduction

Offset curves and surfaces are widely used in many application domains, such as milling and layered manufacturing [1]. The offsets of B-spline and NURBS curves are not rational in general; thus, most CAD systems must rely on approximation techniques for constructing and representing offsets [2,3].

In the last 30 years or so, work on spline approximations for offsets, seeking to get smaller approximation errors, has focused on curve and surface fitting [4,5], equi-volumetric offsets [6,7], level set evolution [8], knot removal [9], and/or detecting singular points [10,11]. Also known are two families of curves that have exact rational offsets. One is the family of *Pythagorean Hodograph (PH) curves*, and the other is the family of *linear normal (LN) curves*.

PH curves were first presented by Farouki [12]. Since then, many approximation methods and properties of the PH curves have been found [13–15] and these have been extended to Pythagorean normal (PN) vector surfaces [16–18].

LN curves have the property that their convolution with NURBS is rational. Quadratic Bézier curves are LN curves. Lee et al. [19] presented an offset approximation based on a quadratic Bézier approximation of circular arcs. Earlier, Lü [20] proved that the offsets of quadratic Bézier curves are rational of degree six using reparametrization. Recently, approximation schemes based on LN curves have been extended to LN surfaces, to approximate offset surfaces [2,21,22].

In this paper, we modify the approximation method of Lee et al. [19]. They presented G^0 and G^1 end-point interpolation methods for offsets. Our method yields a G^2 end-point interpolation and is based on an approximation of circular arcs using quadratic Bézier biarcs. Our approximant is a rational Bézier curve of degree $3d-2$ or $5d-4$ when the initial curve is a Bézier curve or rational Bézier curve of degree d, respectively. We also prove that the Hausdorff distance between two compatible curves, a term defined later, is invariant under convolution. Using this fact, we obtain the exact Hausdorff distance between offset curves and our approximations of them. We also explain an implementation of our approximation scheme and give some numerical examples.

The remainder of this paper is laid out as follows. After some preliminaries have been presented, in Section 2, we give the G^2 end-point interpolation of circular arcs using quadratic Bézier biarcs and derive the Hausdorff distance between two curves. In Section 3, we prove the invariance of Hausdorff distance under convolution and apply it to circle approximation. Then, we explain our algorithm for offset approximation using quadratic Bézier biarcs in Section 4, and present some numerical examples in Section 5. We comment on our approximation method in Section 6.

2. Circle approximation using quadratic Bézier biarcs

Let $\mathbf{c}$ be a circular arc with angle $2\alpha < \pi$, e.g.

$$\mathbf{c}(\theta) = [\cos(\theta), \sin(\theta)] \quad \theta \in [-\alpha, \alpha]. \tag{1}$$

* Corresponding author. Tel.: +82 62 230 7331; fax: +82 62 232 8122.
E-mail address: ahn@chosun.ac.kr (Y.J. Ahn).

0010-4485/$ – see front matter © 2011 Elsevier Ltd. All rights reserved.
doi:10.1016/j.cad.2011.04.005

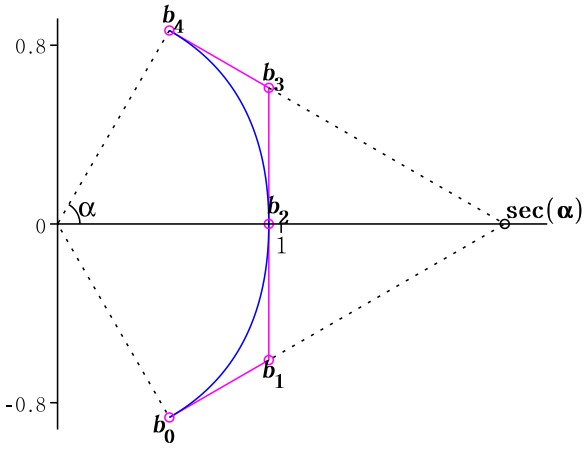

Fig. 1. Piecewise quadratic Bézier biarc (blue) with its control polygon (magenta) $\mathbf{b}_i$, $i = 0, \ldots, 4$, which is a G^2 end-point interpolation of unit circular arc of angle 2α.

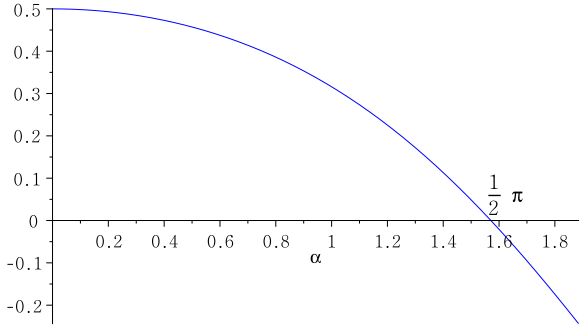

Fig. 2. $m = \frac{\cos(\alpha)}{4}(\sqrt{\cos(\alpha)^2 + 8} - \cos(\alpha)) > 0$ iff $\alpha < \pi/2$.

A quadratic Bézier biarc $\mathbf{c}^a$ can be defined as

$$\mathbf{c}^a(t) = \begin{cases} \sum_{i=0}^{2} \mathbf{b}_i B_i^2(t) & t \in [0, 1] \\ \sum_{i=0}^{2} \mathbf{b}_{i+2} B_i^2(t-1) & t \in (1, 2] \end{cases}$$

where $\mathbf{b}_i$, $i = 0, \ldots, 4$ are the control points and $B_i^2(t)$, $i = 0, 1, 2$ are the quadratic Bernstein polynomials [23]. Our approximation method uses the quadratic Bézier biarc $\mathbf{c}^a$ with the control points

$$\begin{aligned} \mathbf{b}_0 &= [\cos(\alpha), -\sin(\alpha)], \\ \mathbf{b}_1 &= (1-m)[\cos(\alpha), -\sin(\alpha)] + m[\sec(\alpha), 0], \\ \mathbf{b}_2 &= (1-m)[\cos(\alpha), 0] + m[\sec(\alpha), 0], \\ \mathbf{b}_3 &= (1-m)[\cos(\alpha), \sin(\alpha)] + m[\sec(\alpha), 0] \\ \mathbf{b}_4 &= [\cos(\alpha), \sin(\alpha)], \end{aligned} \tag{2}$$

where m is a real number in $(0, 1)$, as shown in Fig. 1. Using the fact [23,24] that the curvature $\kappa(t)$ of the quadratic Bézier curve with control points $\mathbf{b}_0$, $\mathbf{b}_1$, $\mathbf{b}_2$ satisfies

$$\kappa(0) = \frac{\text{area}(\triangle \mathbf{b}_0\mathbf{b}_1\mathbf{b}_2)}{|\Delta \mathbf{b}_0|^3}, \qquad \kappa(1) = \frac{\text{area}(\triangle \mathbf{b}_0\mathbf{b}_1\mathbf{b}_2)}{|\Delta \mathbf{b}_1|^3}$$

where $\Delta \mathbf{b}_k = \mathbf{b}_{k+1} - \mathbf{b}_k$, we find the quadratic Bézier biarc $\mathbf{c}^a$ with a choice of m in Eq. (3) which is a G^2 end-point interpolant of the circular arc, as follows.

Proposition 2.1. *For each $m \in (0, 1)$, the quadratic Bézier biarc $\mathbf{c}^a$ having the control points in Eq. (2) is G^2 continuous at $t = 1$. Moreover, the quadratic Bézier biarc $\mathbf{c}^a$ with the choice of*

$$m = \frac{\cos(\alpha)}{4}(\sqrt{\cos(\alpha)^2 + 8} - \cos(\alpha)) \tag{3}$$

is a unique G^2 end-point interpolation of the circular arc $\mathbf{c}$ in Eq. (1).

Proof. For each $m \in (0, 1)$, the quadratic Bézier biarc $\mathbf{c}^a(t)$, $t \in [0, 2]$ is symmetric with respect to x-axis. Since the three points $\mathbf{b}_1$, $\mathbf{b}_2$ and $\mathbf{b}_3$ are collinear, $\mathbf{c}^a(t)$ is tangent continuous at $t = 1$. Since the curvature $\kappa(t)$ of $\mathbf{c}^a(t)$ satisfies

$$\kappa(1^-) = \frac{\text{area}(\triangle \mathbf{b}_0\mathbf{b}_1\mathbf{b}_2)}{|\Delta \mathbf{b}_1|^3} = \kappa(1) = \frac{\text{area}(\triangle \mathbf{b}_2\mathbf{b}_3\mathbf{b}_4)}{|\Delta \mathbf{b}_2|^3} = \kappa(1^+),$$

so $\mathbf{c}^a(t)$ is curvature continuous at $t = 1$. Also, by the orthogonalities

$$\mathbf{c}^{a\prime}(0) \perp [\cos(\alpha), -\sin(\alpha)], \qquad \mathbf{c}^{a\prime}(2) \perp [\cos(\alpha), \sin(\alpha)],$$

$\mathbf{c}^a(t)$ has the same tangent direction with $\mathbf{c}(\theta)$ at both end-points. Thus, the approximation $\mathbf{c}^a(t)$ is a G^2 end-point interpolation of the circular arc $\mathbf{c}(\theta)$ if and only if it satisfies

$$\kappa(0) = \frac{\text{area}(\triangle \mathbf{b}_0\mathbf{b}_1\mathbf{b}_2)}{|\Delta \mathbf{b}_0|^3} = 1 = \frac{\text{area}(\triangle \mathbf{b}_2\mathbf{b}_3\mathbf{b}_4)}{|\Delta \mathbf{b}_3|^3} = \kappa(2), \tag{4}$$

which is equivalent to

$$4m^4 - (1-m)^2 \cos^4\alpha = 0.$$

This quartic equation has two real roots

$$m = \frac{\cos(\alpha)}{4}(\pm\sqrt{\cos(\alpha)^2 + 8} - \cos(\alpha)),$$

and the choice of m in Eq. (3) is the only real root contained in $(0, 1)$, for $0 < \alpha < \pi/2$, as shown in Fig. 2. □

The *Hausdorff distance* $d_H(C_1, C_2)$ between two curves $C_1(t)$, $t \in [a, b]$ and $C_2(s)$, $s \in [c, d]$ is defined [25,26] by

$$d_H(C_1, C_2) = \max\left\{ \max_{s\in[c,d]} \min_{t\in[a,b]} |C_1(t) - C_2(s)|, \max_{t\in[a,b]} \min_{s\in[c,d]} |C_1(t) - C_2(s)| \right\}.$$

We get the Hausdorff distance $d_H(\mathbf{c}, \mathbf{c}^a)$ as follows.

Proposition 2.2. *The Hausdorff distance between $\mathbf{c}$ and $\mathbf{c}^a$ with the choice of m in Eq. (3) is*

$$d_H(\mathbf{c}, \mathbf{c}^a) = 1 - \cos(\alpha) + \frac{1}{4}\sin^2(\alpha)(\cos(\alpha) - \sqrt{\cos^2(\alpha) + 8}).$$

Its approximation order is four.

Proof. Both curves $\mathbf{c}(\theta)$ and $\mathbf{c}^a(t)$ are symmetric with respect to x-axis. It is sufficient to find the maximum of the function

$$\psi(t) = ||\mathbf{c}^a(t)| - 1| = |\sqrt{x(t)^2 + y(t)^2} - 1|$$

in the half interval $[0, 1]$, where $[x(t), y(t)] = \mathbf{c}^a(t)$. Note that $\psi'(t) = 0$ if and only if

$$x'(t)x(t) + y'(t)y(t) = 0.$$

Since

$$\begin{aligned} x'(t)x(t) + y'(t)y(t) = \frac{3}{4}\sin^2(\alpha)(&\cos(\alpha)^4 + 7\cos^2(\alpha) \\ &+ 4 - \cos(\alpha)(\cos(\alpha)^2 + 3)\sqrt{\cos(\alpha)^2 + 8}) \cdot t^2(t-1), \end{aligned}$$

$\psi(t)$ has critical points at $t = 0, 1$, and so it reaches the maximum at $t = 1$. Thus, we have

$$\begin{aligned} d_H(\mathbf{c}, \mathbf{c}^a) = \psi(1) = 1 - \cos(\alpha) + \frac{1}{4}\sin^2(\alpha)(&\cos(\alpha) \\ &- \sqrt{\cos^2(\alpha) + 8}). \end{aligned}$$

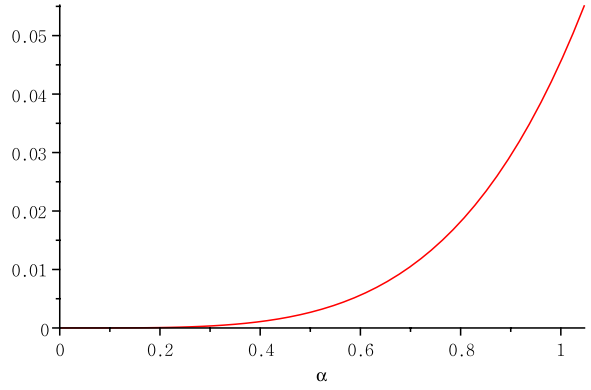

Fig. 3. $d_H(\mathbf{c}, \mathbf{c}^a) = \epsilon(\alpha) = 1 - \cos(\alpha) + \frac{1}{4}\sin^2(\alpha)(\cos(\alpha) - \sqrt{\cos^2(\alpha) + 8})$.

By series expansion, we obtain

$$d_H(\mathbf{c}, \mathbf{c}^a) = \frac{1}{24}\alpha^4 + \mathcal{O}(\alpha^6)$$

whose approximation order is four. □

The Hausdorff distance $d_H(\mathbf{c}, \mathbf{c}^a)$ between the unit circular arc $\mathbf{c}$ of angle 2α and its quadratic Bézier biarc approximation $\mathbf{c}^a$ with the choice of m in Eq. (3) depends only on the angle α. We denote it by $\epsilon(\alpha)$ and plot it in Fig. 3.

3. Hausdorff distance and convolution

In this section, we prove that the Hausdorff distance of two regular compatible curves is invariant under convolution with the same planar curve.

For the regular planar curve $C(t) = [x(t), y(t)]$, $t \in [a, b]$, the unit normal vector field is defined by $N(C(t)) = [-y'(t), x'(t)]/\sqrt{x'(t)^2 + y'(t)^2}$, and the graph of $N(C(t))$, $t \in [a, b]$, is called the *Gauss map* $\mathcal{N}(C)$. If two regular planar curves $\mathbf{C}_1(t)$ and $\mathbf{C}_2(s)$ have the same Gauss map, then they are *compatible*.

If two compatible curves satisfy

$$C_1'(t) \parallel C_2'(s(t)) \quad \text{and} \quad \langle C_1'(t), C_2'(s(t))\rangle > 0$$

for a reparametrization $s = s(t)$, then the *convolution curve* $C_1 * C_2$ is defined by

$$(C_1 * C_2)(t) = C_1(t) + C_2(s(t)),$$

as illustrated in Fig. 4. For more information about convolution curves or Gauss maps, see, e.g., [19,27–30].

Let two regular planar curves $\mathbf{b}$ and $\mathbf{p}$ be compatible with no inflection point and a range of the Gauss map of less than π. If $\mathbf{q}$ is an end-point interpolation of the planar curve $\mathbf{p}$, and if $\mathbf{q}$ and $\mathbf{b}$ are compatible, then there are reparametrizations $t = t(u)$ and $s = s(u)$ satisfying

$$\mathbf{b}'(u) \parallel \mathbf{p}'(s(u)) \parallel \mathbf{q}'(t(u)) \tag{5}$$

for each u.

Let $\bar{\mathbf{p}}(u) = \mathbf{p}(s(u))$ and $\bar{\mathbf{q}}(u) = \mathbf{q}(t(u))$ for each u, and let $L_{\bar{\mathbf{p}}}(u)$ and $L_{\bar{\mathbf{q}}}(u)$ be the tangent lines of $\bar{\mathbf{p}}(u)$ and $\bar{\mathbf{q}}(u)$, respectively. We have the convolution curves

$$\begin{aligned}(\mathbf{b} * \mathbf{p})(u) &= \mathbf{b}(u) + \mathbf{p}(s(u)) = \mathbf{b}(u) + \bar{\mathbf{p}}(u)\\ (\mathbf{b} * \mathbf{q})(u) &= \mathbf{b}(u) + \mathbf{q}(t(u)) = \mathbf{b}(u) + \bar{\mathbf{q}}(u)\end{aligned} \tag{6}$$

as shown in Fig. 5. Their derivatives are $(\mathbf{b} * \mathbf{p})'(u) = \mathbf{b}'(u) + \bar{\mathbf{p}}'(u)$ and $(\mathbf{b} * \mathbf{q})'(u) = \mathbf{b}'(u) + \bar{\mathbf{q}}'(u)$.

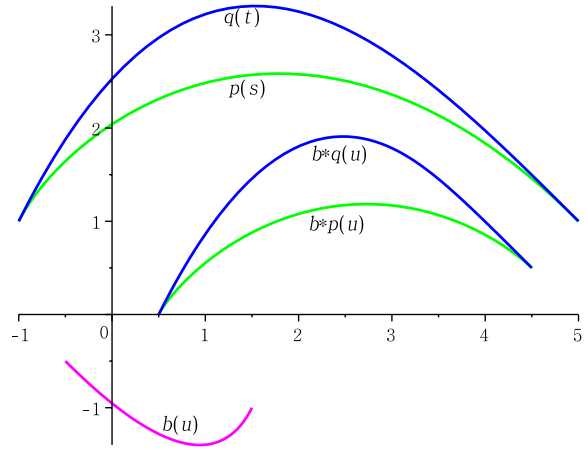

Fig. 5. Convolution curves $\mathbf{b} * \mathbf{p}(u)$ and $\mathbf{b} * \mathbf{q}(u)$.

Lemma 3.1. *Let two regular planar curves* $\mathbf{b}$ *and* $\mathbf{p}$ *be compatible with no inflection point and with the norm of the Gauss map less than* π. *If* $\mathbf{q}$ *is an end-point interpolation of the plane curve* $\mathbf{p}$, *and if* $\mathbf{q}$ *and* $\mathbf{b}$ *are compatible, then for each* u

$$d_H(L_{\bar{\mathbf{p}}}(u), L_{\bar{\mathbf{q}}}(u)) = d_H(L_{\mathbf{b}*\mathbf{p}}(u), L_{\mathbf{b}*\mathbf{q}}(u)).$$

Proof. For each u, the tangent vectors of $(\mathbf{b} * \mathbf{p})(u)$ and $(\mathbf{b} * \mathbf{q})(u)$ have the same direction, namely $\mathbf{b}'(u) + \bar{\mathbf{p}}'(u)$ and $\mathbf{b}'(u) + \bar{\mathbf{q}}'(u)$. Thus, $(\mathbf{b} * \mathbf{p})'(u)$ is parallel to $(\mathbf{b} * \mathbf{q})'(u)$, and so they are parallel to $\bar{\mathbf{p}}'(u)$ and $\bar{\mathbf{q}}'(u)$ by Eq. (5). Hence,

$$L_{\mathbf{b}*\mathbf{p}}(u) \parallel L_{\mathbf{b}*\mathbf{q}}(u) \parallel L_{\bar{\mathbf{p}}}(u) \parallel L_{\bar{\mathbf{q}}}(u).$$

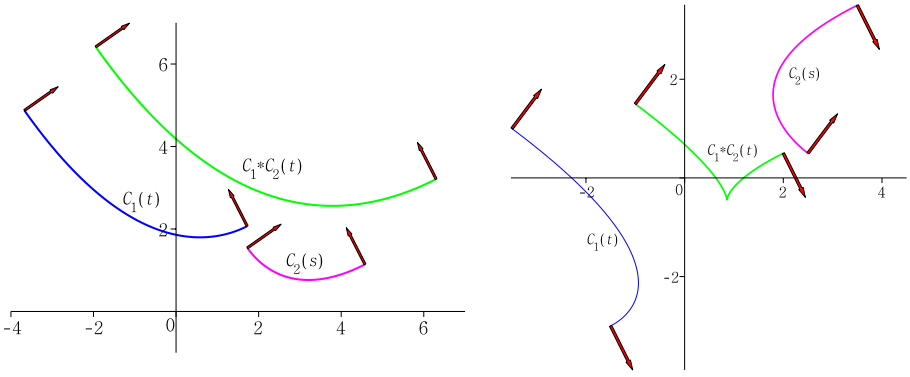

Fig. 4. Convolution curve $(C_1 * C_2)(t)$ of the compatible curves $C_1(t)$ and $C_2(s)$.

By Eq. (6), $L_{\mathbf{b}*\mathbf{p}}(u)$ and $L_{\mathbf{b}*\mathbf{q}}(u)$ are the translated lines of $L_{\bar{\mathbf{p}}}(u)$ and $L_{\bar{\mathbf{q}}}(u)$, by $\mathbf{b}(u)$, as shown in Fig. 6. Hence,

$$d_H(L_{\bar{\mathbf{p}}}(u), L_{\bar{\mathbf{q}}}(u)) = d_H(L_{\mathbf{b}*\mathbf{p}}(u), L_{\mathbf{b}*\mathbf{q}}(u)). \quad \square$$

Proposition 3.2. *If* $\mathbf{b}$, $\mathbf{p}$ *and* $\mathbf{q}$ *satisfy the hypotheses of Lemma 3.1, then*

$$d_H(\mathbf{p}, \mathbf{q}) = \max_u \{d_H(L_{\bar{\mathbf{p}}}(u), L_{\bar{\mathbf{q}}}(u))\}.$$

Proof. For any u_0, $L_{\bar{\mathbf{p}}}(u_0)$ and $L_{\bar{\mathbf{q}}}(u_0)$ are parallel and are the tangent lines of $\bar{\mathbf{p}}(u)$ and $\bar{\mathbf{q}}(u)$ at $u = u_0$, respectively. Since $\bar{\mathbf{p}}(u)$ and $\bar{\mathbf{q}}(u)$ are regular convex and the norms of their Gauss maps are less than π, we have

$$d_H(L_{\bar{\mathbf{p}}}(u_0), L_{\bar{\mathbf{q}}}(u_0)) \le \max\{d_H(\bar{\mathbf{p}}(u_0), \bar{\mathbf{q}}), d_H(\bar{\mathbf{p}}, \bar{\mathbf{q}}(u_0))\}.$$

Since $d_H(\bar{\mathbf{p}}(u_0), \bar{\mathbf{q}}) = d_H(\bar{\mathbf{p}}(u_0), \mathbf{q})$ and $d_H(\bar{\mathbf{p}}, \bar{\mathbf{q}}(u_0)) = d_H(\mathbf{p}, \bar{\mathbf{q}}(u_0))$, we have

$$\max\{d_H(\bar{\mathbf{p}}(u_0), \bar{\mathbf{q}}), d_H(\bar{\mathbf{p}}, \bar{\mathbf{q}}(u_0))\} = \max\{d_H(\bar{\mathbf{p}}(u_0), \mathbf{q}), d_H(\mathbf{p}, \bar{\mathbf{q}}(u_0))\} \le d_H(\mathbf{p}, \mathbf{q}).$$

Thus, $d_H(L_{\bar{\mathbf{p}}}(u), L_{\bar{\mathbf{q}}}(u)) \le d_H(\mathbf{p}, \mathbf{q})$ for each u, so that

$$\max_u \{d_H(L_{\bar{\mathbf{p}}}(u), L_{\bar{\mathbf{q}}}(u))\} \le d_H(\mathbf{p}, \mathbf{q}). \tag{7}$$

Conversely, assume that $\bar{\mathbf{p}}(\tilde{u})$ and $\bar{\mathbf{q}}(\hat{u})$ are the points that determine the Hausdorff distance between two curves $\mathbf{p}$ and $\mathbf{q}$, i.e.,

$$d_H(\mathbf{p}, \mathbf{q}) = d_H(\bar{\mathbf{p}}(\tilde{u}), \bar{\mathbf{q}}(\hat{u})).$$

Since $\mathbf{p}$ and $\mathbf{q}$ are compatible and have no cusp, the two points $\bar{\mathbf{p}}(\tilde{u})$ and $\bar{\mathbf{q}}(\hat{u})$ satisfy

$$\bar{\mathbf{p}}'(\tilde{u}) \circ (\bar{\mathbf{p}}(\tilde{u}) - \bar{\mathbf{q}}(\hat{u})) \quad \text{and} \quad \bar{\mathbf{q}}'(\hat{u}) \circ (\bar{\mathbf{p}}(\tilde{u}) - \bar{\mathbf{q}}(\hat{u}))$$

as shown in Fig. 7. Thus, $L_{\bar{\mathbf{p}}(\tilde{u})} \parallel L_{\bar{\mathbf{q}}(\hat{u})}$ and so $\hat{u} = \tilde{u}$. Hence,

$$d_H(\mathbf{p}, \mathbf{q}) = d_H(\bar{\mathbf{p}}(\tilde{u}), \bar{\mathbf{q}}(\hat{u})) = d_H(L_{\bar{\mathbf{p}}}(\hat{u}), L_{\bar{\mathbf{q}}}(\tilde{u})) \le \max_u \{d_H(L_{\bar{\mathbf{p}}}(u), L_{\bar{\mathbf{q}}}(u))\}. \tag{8}$$

Eqs. (7) and (8) yield

$$d_H(\mathbf{p}, \mathbf{q}) = \max_u \{d_H(L_{\bar{\mathbf{p}}}(u), L_{\bar{\mathbf{q}}}(u))\}. \quad \square$$

Theorem 3.3. *If* $\mathbf{b}$, $\mathbf{p}$ *and* $\mathbf{q}$ *satisfy the hypotheses of Lemma 3.1 and* $\mathbf{b} * \mathbf{p}$ *and* $\mathbf{b} * \mathbf{q}$ *have no cusp, then*

$$d_H(\mathbf{b} * \mathbf{p}, \mathbf{b} * \mathbf{q}) = d_H(\mathbf{p}, \mathbf{q}).$$

Proof. By Proposition 3.2 and by the regularity of $\mathbf{b} * \mathbf{p}$ and $\mathbf{b} * \mathbf{q}$,

$$d_H(\mathbf{p}, \mathbf{q}) = \max_u \{d_H(L_{\bar{\mathbf{p}}}(u), L_{\bar{\mathbf{q}}}(u))\},$$

$$d_H(\mathbf{b} * \mathbf{p}, \mathbf{b} * \mathbf{q}) = \max_u \{d_H(L_{\mathbf{b}*\mathbf{p}}(u), L_{\mathbf{b}*\mathbf{q}}(u))\}.$$

By the Lemma 3.1,

$$d_H(L_{\bar{\mathbf{p}}}(u), L_{\bar{\mathbf{q}}}(u)) = d_H(L_{\mathbf{b}*\mathbf{p}}(u), L_{\mathbf{b}*\mathbf{q}}(u))$$

for each u. Therefore, we obtain

$$d_H(\mathbf{b} * \mathbf{p}, \mathbf{b} * \mathbf{q}) = d_H(\mathbf{p}, \mathbf{q}). \quad \square$$

The result of Theorem 3.3 can be used to find the Hausdorff distance between an offset curve $\mathbf{b} * r\mathbf{c}$ and its approximation $\mathbf{b} * r\mathbf{c}^a$ for the given planar regular curve $\mathbf{b}$ and offset distance $r \in \mathbb{R}$, where $\mathbf{c}$ is the unit circular arc compatible with $\mathbf{b}$ and $\mathbf{c}^a$ is the quadratic Bézier biarc approximation of $\mathbf{c}$ presented in Section 2.

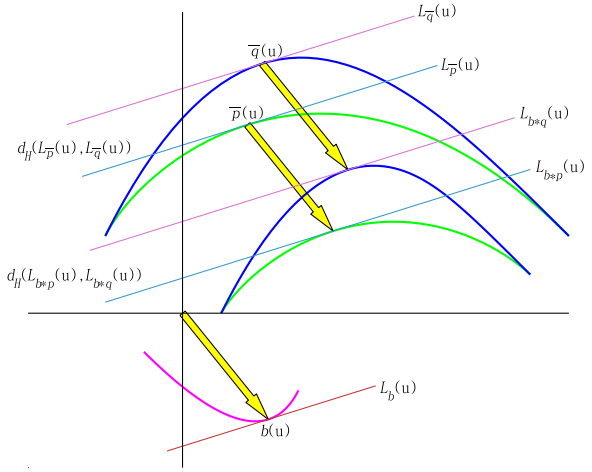

Fig. 6. $d_H(L_{\bar{\mathbf{p}}}(u), L_{\bar{\mathbf{q}}}(u)) = d_H(L_{\mathbf{b}*\mathbf{p}}(u), L_{\mathbf{b}*\mathbf{q}}(u))$, for each u.

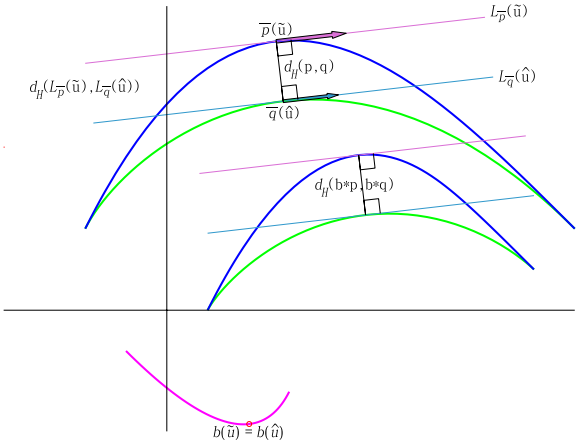

Fig. 7. Hausdorff distances $d_H(\mathbf{p}, \mathbf{q})$ and $d_H(\mathbf{b} * \mathbf{p}, \mathbf{b} * \mathbf{q})$.

Corollary 3.4. *Let* $\mathbf{b}$ *be a planar regular curve with a norm of the Gauss map less than* π. *Let* $\mathbf{c}$ *be the circular arc compatible with* $\mathbf{b}$ *and* $\mathbf{c}^a$ *the quadratic Bézier biarc* G^2 *end-point interpolation. If* $\mathbf{b} * r\mathbf{c}$ *and* $\mathbf{b} * r\mathbf{c}^a$ *have no cusp except possibly at the end-points, then*

$$d_H(\mathbf{b} * r\mathbf{c}, \mathbf{b} * r\mathbf{c}^a) = r \cdot d_H(\mathbf{c}, \mathbf{c}^a). \tag{9}$$

Proof. If $\mathbf{b} * r\mathbf{c}$ and $\mathbf{b} * r\mathbf{c}^a$ have no cusp including both end points, then by Theorem 3.3 we obtain Eq. (9). Even if $\mathbf{b} * r\mathbf{c}$ and $\mathbf{b} * r\mathbf{c}^a$ have a cusp at one or both end points, since the end points of $\mathbf{b} * r\mathbf{c}$ and $\mathbf{b} * r\mathbf{c}^a$ coincide, the assertion follows. $\square$

In the thesis of the third author, Kim [31], similar results have been obtained about quadratic Bézier curves. They are extended in this work to regular curves.

4. Approximation method for offset curves and algorithm

In this section, we present a method for curvature continuous offset approximation based on the circle approximation using quadratic Bézier biarcs, and present our algorithm for the approximation. Our method is a modification of Lee's method [19] which uses quadratic Bézier curves for circle approximation, while our method uses quadratic Bézier biarcs to achieve G^2 end-point interpolation.

Let $\mathbf{b}(u)$ be the given planar regular parametric curve such as a B-spline or NURBS curve, $u \in [b_0, b_1]$, and let $r \in \mathbb{R}$ be the offset distance.

First, the given curve should be subdivided at the inflection points, since a quadratic Bézier biarc cannot have inflection points. Also, the curve $\mathbf{b}(u)$ should be subdivided at the points where the signed curvature $\kappa(u)$ is $-1/r$, so that the convolution $\mathbf{b} * r\mathbf{c}$ has no cusp in the domain interior and Corollary 3.4 can be applied. Let N be the number of these subdivisions, and $t_i \in (b_0, b_1), i = 1, \ldots, N$ be the subdivision point. Put $t_0 = b_0$ and $t_{N+1} = b_1$.

Now, for each segment, let α_i be the half norm of the Gauss map $\mathcal{N}(\mathbf{b}(u))$, $u \in [t_{i-1}, t_i]$. We find the smallest positive integer K_i satisfying

$$\epsilon\left(\frac{\alpha_i}{K_i}\right) < \frac{TOL}{r} \tag{10}$$

where TOL is the prescribed tolerance. Then each segment $\mathbf{b}(u)$, $u \in [t_i, t_{i+1}]$, is subdivided into K_i smaller segments. In all, the curve is subdivided into

$$\sum_{i=0}^{N} K_i$$

segments. For each i, we find $t_{ij} \in [t_i, t_{i+1}]$, $j = 0, \ldots, 2K_i$ satisfying

$$N(\mathbf{b}(t_{ij})) = \frac{j}{2K_i} \cdot N(\mathbf{b}(t_i)) + \left(1 - \frac{j}{2K_i}\right) \cdot N(\mathbf{b}(t_{i+1}))$$

and compute the unit circular arc $\mathbf{c}(\theta)$ and its G^2 quadratic biarc approximant $\mathbf{c}^a(t)$, compatible with the segment $\mathbf{b}(u)$, $u \in [t_{i,2j}, t_{i,2j+2}], j = 0, \ldots, K_{i-1}$. By Eq. (10) and the definition of $\epsilon(\alpha)$, we have

$$d_H(\mathbf{c}, \mathbf{c}^a) < \frac{TOL}{r}. \tag{11}$$

For each $i = 0, \ldots, N$ and $j = 0, \ldots, 2K_i - 1$, we can obtain the convolution curve $(\mathbf{b} * r\mathbf{c}^a)(u) = \mathbf{b}(u) + \mathbf{c}^a(t(u))$ using the reparametrization $t = t(u)$ satisfying

$$\mathbf{b}'(u) \parallel \mathbf{c}^{a\prime}(t)$$

in $[t_{i,j}, t_{i,j+1}]$. Since $\mathbf{c}^a(t)$ is a quadratic Bézier curve, $t(u)$ is rational of degree $d - 1$ or $2d - 2$, and $(\mathbf{b} * r\mathbf{c}^a)(u)$ is a rational curve of degree $3d-2$ or $5d-4$, when $\mathbf{b}(u)$ is a B-spline or NURBS of degree d, respectively [19].

For $i = 0, \ldots, N$ and $j = 0, \ldots, K_i$, all points $(\mathbf{b} * r\mathbf{c}^a)(t_{i,2j})$ lie on the offset curve $\mathbf{b} * r\mathbf{c}$. Let U be the set of all knots of the spline $\mathbf{b}(u)$ in (b_0, b_1). For each j, if there is no knot in the open interval $(t_{i,j}, t_{i,j+1})$, then $(\mathbf{b} * r\mathbf{c}^a)(u)$ is one rational Bézier curve segment in the interval. But if there is a knot in the open interval $(t_{i,j}, t_{i,j+1})$, then $(\mathbf{b} * r\mathbf{c}^a)(u)$ consists of two rational Bézier curve segments in the interval. Thus, the total number of segments of $(\mathbf{b} * r\mathbf{c}^a)(u)$, $u \in [b_0, b_1]$ is

$$2\sum_{i=0}^{N} K_i + m$$

where m is the number of knots in the open interval (b_0, b_1) that are not equal to $t_{i,j}$, $i = 0, \ldots, N, j = 0, \ldots, 2K_i$.

Finally, the rational spline curve $(\mathbf{b} * r\mathbf{c}^a)(u), u \in [b_0, b_1]$ is the approximation of the offset curve $(\mathbf{b} * r\mathbf{c})(u)$ and

$$d_H(\mathbf{b} * r\mathbf{c}, \mathbf{b} * r\mathbf{c}^a) = r \cdot d_H(\mathbf{c}, \mathbf{c}^a) < TOL$$

by Eq. (11) and Corollary 3.4. Also by Proposition 2.1, the approximant $(\mathbf{b} * r\mathbf{c}^a)(u)$ is curvature continuous except for the cusps. The signed curvature of $(\mathbf{b} * r\mathbf{c}^a)(u)$ interpolates that of $(\mathbf{b} * r\mathbf{c})(u)$ at $u = t_{i,2j}, i = 0, \ldots, N$ and $j = 0, \ldots, K_i$. We present the algorithm for G^2 end-point interpolation of offset curve of given curve $\mathbf{b}(u)$ using rational curve $(\mathbf{b} * r\mathbf{c}^a)(u)$.

ALGORITHM

input : $\mathbf{b}(u)$, $[b_0, b_1]$, U, r, TOL.
find $t_i \in (b_0, b_1)$, $i = 1, \cdots, N$ satisfying $\kappa(t_i) = 0$ or $-1/r$.
set $t_0 = b_0, t_{N+1} = b_1$
for i from 0 to N do
  subdivide $\mathbf{b}(u)$ into $[t_i, t_{i+1}]$
  let α_i be the half norm of $\mathcal{N}(\mathbf{b}, [t_i, t_{i+1}])$
  let K_i be the smallest positive integer satisfying $\epsilon(\frac{\alpha_i}{K_i}) < TOL$
  find $t_{ij}, j = 0, \cdots, 2K_i$ such that

$$N(\mathbf{b}(t_{i,j})) = \frac{j}{2K_i} \cdot N(\mathbf{b}(t_i)) + (1 - \frac{j}{2K_i}) \cdot N(\mathbf{b}(t_{i+1}))$$

  for j from 0 to $K_i - 1$ do
    find the quadratic Bézier biarc approximation $\mathbf{c}^a(t)$ which is compatible with $\mathbf{b}(u)$, $u \in [t_{i,2j}, t_{i,2j+2}]$
    let $m_{i,j}$ be the number of knots in $(t_{i,2j}, t_{i,2j+2}) - \{t_{i,2j+1}\}$
    put $s_0^{i,j} = t_{i,2j}$ and $s_{m_{i,j}+2}^{i,j} = t_{i,2j+2}$
    let $s_k^{i,j}$ be the elements of $(U \cap (t_{i,2j}, t_{i,2j+2})) \cup \{t_{i,2j+1}\}$ for $k = 1, \cdots, m_{i,j} + 1$, in increasing order
    for k from 0 to $m_{i,j} + 1$ do
      find $t = t(u)$ satisfying $\mathbf{b}'(u) \parallel \mathbf{c}^{a\prime}(t)$, $u \in [s_k^{i,j}, s_{k+1}^{i,j}]$
      calculate $(\mathbf{b} * r\mathbf{c}^a)_{i,j,k}(u) = \mathbf{b}(u) + r\mathbf{c}^a(t(u))$, $u \in [s_k^{i,j}, s_{k+1}^{i,j}]$
    end do
  end do
end do
set $m = \sum_{i=0}^{N} \sum_{j=0}^{K_i - 1} m_{i,j}$
output : $N, K_i, m_{i,j}, (\mathbf{b} * r\mathbf{c}^a)_{i,j,k}(u), s_k^{i,j}$

5. Numerical examples

We apply our approximation method to examples that were presented by Lee et al. [19], as shown in Figs. 8–10. The initial curve $\mathbf{b}(u)$ in Figs. 8–10, is a uniform cubic B-spline, a cubic Bézier curve, and a quadratic NURBS curve, to be offset by $r = 0.5$, 1 and 0.6, respectively. They are all curvature continuous.

The cubic B-spline in Fig. 8 has four inflection points and two points satisfying $\kappa(u) = -1/r$ for $r = 0.5$. So, the curve is subdivided into seven pieces $\mathbf{b}(u)$, $u \in [t_i, t_{i+1}]$, $i = 0, \ldots, 6$, and $N = 6$. The cubic Bézier curve and the quadratic NURBS in Figs. 9 and 10 have no inflection points and no points satisfying $\kappa(u) = -1/r$ for $r = 1$ and 0.6, so in that case $N = 0$.

In Fig. 8, there are three knots which are not equal to any $t_{i,j}$, so $m = 3$, in Fig. 9, there is no interior knot, $m = 0$, and in Fig. 10, at most three knots are contained in some open interval $(t_{i,j}, t_{i,j+1})$, thus $m \leq 3$.

In the examples of Figs. 8 and 9, $\mathbf{b}$ is a cubic curve, and so $(\mathbf{b} * r\mathbf{c}^a)$ is a rational curve of degree seven. In the case of quadratic NURBS, $(\mathbf{b} * r\mathbf{c}^a)$ is a rational curve of degree six. Using our algorithm, we get the approximant $(\mathbf{b} * r\mathbf{c}^a)(u)$ which is curvature continuous except for the cusps, as shown in Fig. 8(c)–Fig. 10(c).

Table 1 was first presented by Lee et al. [19]. They implemented the approximation methods of Cobb (*Cob*), Elber and Cohen (*Elb* and *Elb*2), Tiller and Hanson (*Til*), an extension of Hoschek and

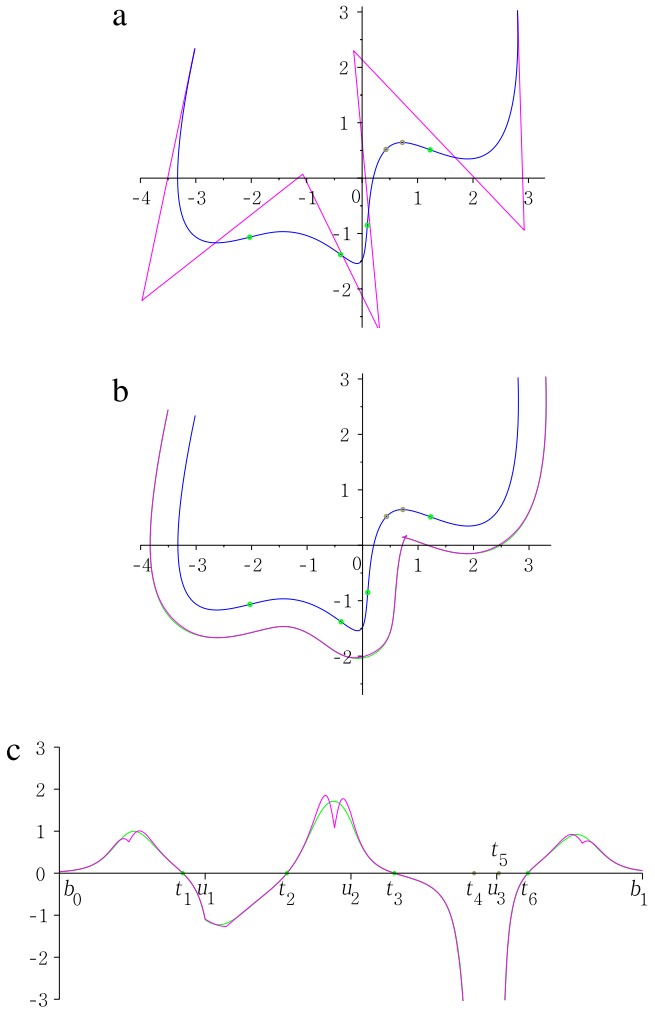

Fig. 8. (a) Uniform cubic B-spline (blue) curve $\mathbf{b}(u)$ and its control polygon (magenta). The inflection points (small green circles) satisfy $\kappa(u) = 0$ and the points where the offset has a cusp (small khaki circle) satisfy $\kappa(u) = -1/r$ for $r = 0.5$. (b) The offset curve(green) $\mathbf{b} * r\mathbf{c}$ and its approximation (magenta) $\mathbf{b} * r\mathbf{c}^a$, for $TOL = 0.1$. (c) The signed curvature $\kappa_{\mathbf{b}*r\mathbf{c}}(u)$ (green) and $\kappa_{\mathbf{b}*r\mathbf{c}^a}(u)$ (magenta). $U = \{u_1, u_2, u_3\}$ is interior knot vector in (b_0, b_1). (For interpretation of the references to colour in this figure legend, the reader is referred to the web version of this article.)

Wissel's method (*Lst* and *Lst*2), and their method (*Lee*). They also compared the results obtained from these methods as shown in Table 1, which shows the number of control points for the error within the given tolerance *TOL*. Later, Piegl and Tiller[9] added the result from their method (*P*&*T*). The last column in Table 1 is the results by our approximation method.

The numbers in Table 1 show that the methods of *Lst*, *Lst*2, *Lee* and *P*&*T* are better than our method. But our method has some merits which other methods do not have, e.g., G^2 end-point interpolation of offset curves and a-priori error analysis.

6. Conclusions

In this paper, we showed that the Hausdorff distance between two compatible curves is invariant under convolution when these have no cusp in their domain interior. Using this fact and the circle approximation by quadratic Bézier biarcs, we presented a method for G^2 end-point interpolation of offset curves by rational Bézier curves.

Our approximation method has two merits. One is that a-priori error analysis can be obtained due to Theorem 3.3, so we can determine the number of subdivisions needed to achieve an approximation within a prescribed error tolerance. The other advantage of our method is that the curvature of our approximation interpolates the curvature of the offset curve for all subdivision points and both end points.

In future work, we plan to consider circle approximations using LN curves of high degree with high order of contact at both end points. Based on this approximation and using Theorem 3.3, high-order approximation of offset curves by rational curves could be obtained.

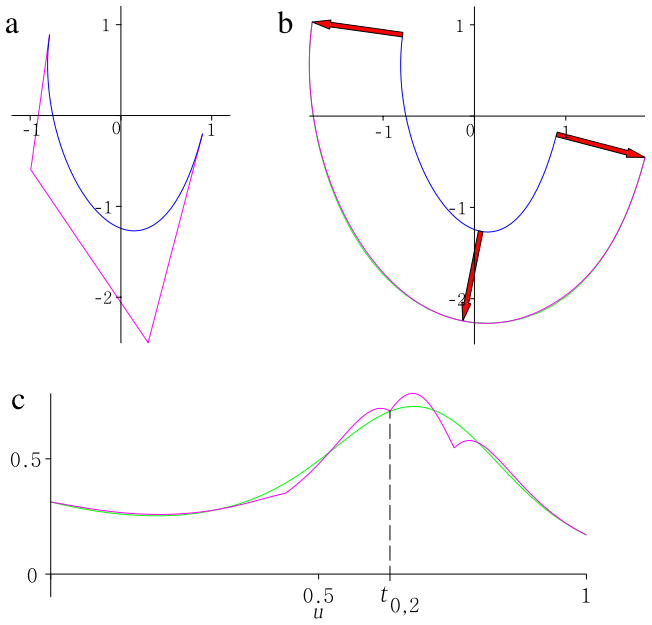

Fig. 9. (a) Cubic Bézier (blue) curve $\mathbf{b}(u)$ and its control polygon (magenta). (b) The offset curve (green) $\mathbf{b}*\mathbf{c}(u)$ and its approximation (magenta) $\mathbf{b}*\mathbf{c}^a(u)$, for $TOL = 0.1$. The true Hausdorff distance is 1.44×10^{-2}. The (red) arrows are unit normal vectors at end points and subdivision points. (c) The signed curvature $\kappa_{\mathbf{b}*\mathbf{c}}(u)$ (green) and $\kappa_{\mathbf{b}*\mathbf{c}^a}(u)$ (magenta). (For interpretation of the references to colour in this figure legend, the reader is referred to the web version of this article.)

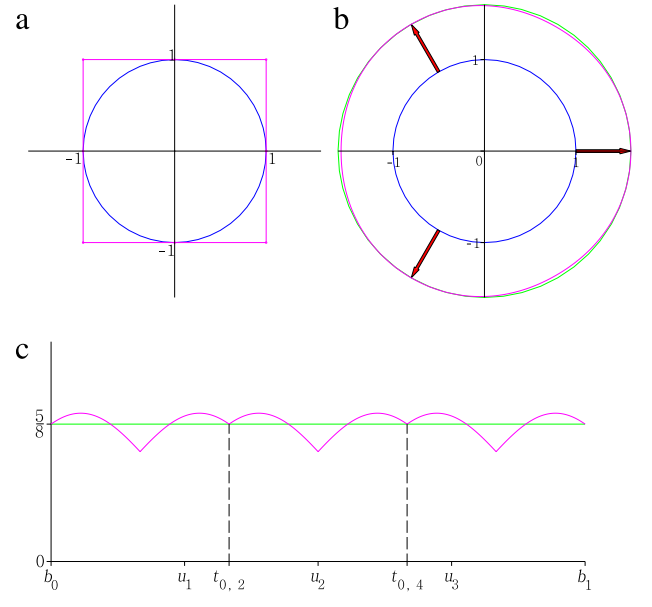

Fig. 10. (a) Quadratic NURBS (blue) curve $\mathbf{b}(u)$ which represents unit circle and its control polygon (magenta). (b) The offset curve(green) $\mathbf{b} * \mathbf{c}(u)$ and its approximation (magenta) $\mathbf{b} * \mathbf{c}^a(u)$, for $TOL = 0.1$. (c) The signed curvature $\kappa_{\mathbf{b}*\mathbf{c}}(u)$ (green) and $\kappa_{\mathbf{b}*\mathbf{c}^a}(u)$ (magenta). $U = \{u_1, u_2, u_3\}$. (For interpretation of the references to colour in this figure legend, the reader is referred to the web version of this article.)

Table 1
Number of control points of spline approximant curves with their errors less than given tolerance *TOL* for the offset curve of (a) cubic B-spline in Fig. 8, (b) cubic Bézier curve in Fig. 9, and (c) quadratic NURBS in Fig. 10. Piegl and Tiller (*P&T*)[9] did not present the result in (c).

TOL	*Cob*	*Elb*	*Elb2*	*Til*	*Lst*	*Lst2*	*Lee*	*P&T*	Our method
(a)									
10^{-1}	28	19	22	25	16	31	78	19	120
10^{-2}	73	57	55	67	48	49	92	33	162
10^{-3}	208	174	190	202	84	94	120	56	232
10^{-4}	637	417	550	640	138	166	176	101	330
10^{-5}	1846	1357	1690	1918	240	277	302	179	568
(b)									
10^{-1}	10	11	13	10	7	10	22	6	29
10^{-2}	31	24	25	31	13	19	29	9	43
10^{-3}	94	74	97	97	19	31	43	15	71
10^{-4}	316	216	247	322	31	46	71	25	113
10^{-5}	865	974	769	886	50	88	127	43	183
TOL	*Cob*	*Elb*	*Elb2*	*Til*	*Lst*	*Lst2*	*Lee*	Our method	
(c)									
10^{-1}	17	13	11	9	9	9	25	49	
10^{-2}	33	53	27	9	13	17	49	73	
10^{-3}	129	69	123	9	24	33	73	97	
10^{-4}	513	261	299	9	46	65	121	169	
10^{-5}	1025	524	1019	9	98	117	199	289	

Acknowledgments

This research was supported by Basic Science Research Program through the National Research Foundation of Korea(NRF) funded by the Ministry of Education, Science and Technology (2011-0010147); by grants CPATH 0722210 and CPATH 0938999 of the US National Science Foundation; and by a gift from the Intel Corporation. The authors are grateful to the editor and five anonymous referees for their valuable comments and constructive suggestions.

References

[1] Jüttler B, Sampoli ML. Hermite interpolation by piecewise polynomial surfaces with rational offsets. Comput Aided Geom Design 2000;17:361–85.
[2] Bastl B, Jüttler B, Kosinka J, Lávička M. Computing exact rational offsets of quadratic triangular Bézier surface patches. Comput Aided Design 2008;40:197–209.
[3] Elber G, Cohen E. Error bounded variable distance offset perator for free form curves and surfaces. Internat J Comput Geom Appl 1991;1:67–78.
[4] Hoschek J, Wissel N. Optimal approximate conversion of spline curves and spline approximation of offset curves. Comput Aided Design 1988;20:475–483.
[5] Pottmann H, Leopoldseder S. A concept for parametric surface fitting which avoids the parametrization problem. Comput Aided Geom Design 2003;20:343–62.
[6] Moon HP. Equivolumetric offsets for 2D machining with constant material removal rate. Comput Aided Geom Design 2008;25:397–410.
[7] Moon HP. Equivolumetric offset surfaces. Comput Aided Geom Design 2009;26:17–36.
[8] Kimmel R, Bruckstein AM. Shape offsets via level sets. Comput Aided Design 1993;25:154–62.
[9] Piegl L, Tiller W. Computing offsets of NURBS curves and surfaces. Comput Aided Design 1999;31:147–56.
[10] Seong JK, Elber G, Kim M-S. Trimming local and global self-intersections in offset curves/surfaces using distance maps. Comput Aided Design 2006;38:183–93.
[11] Seong JK, Johnson DE, Elber G, Cohen E. Critical point analysis using domain lifting for fast geometry queries. Comput Aided Design 2010;42:613–24.
[12] Farouki RT, Sakkalis T. Pythagorean hodographs. IBM J Res Dev 1990;34:736–52.
[13] Choi HI, Farouki RT, Kwon S-H, Moon HP. Topological criterion for selection of quintic Pythagorean-hodograph Hermite interpolants. Comput Aided Geom Design 2008;25:411–33.
[14] Farouki RT, Sederberg TW. Analysis of the offset to a parabola. Comput Aided Geom Design 1995;12(6):639–45.
[15] Šír Z, Bastl B, Lávička M. Hermite interpolation by hypocycloids and epicycloids with rational offsets. Comput Aided Geom Design 2010;27:405–17.
[16] Lávička M, Bastl B. PN surfaces and their convolutions with rational surfaces. Comput Aided Geom Design 2008;25:763–74.
[17] Peternell M, Pottmann H. A laguerre geometric approach to rational offsets. Comput Aided Geom Design 1998;15:223–49.
[18] Pottmann H. Rational curves and surfaces with rational offsets. Comput Aided Geom Design 1995;12:175–92.
[19] Lee IK, Kim M-S, Elber G. Planar curve offset based on circle approximation. Comput Aided Design 1996;28:617–30.
[20] Lü W. Rational offsets by reparametrizations, preprint, 1992.
[21] Aigner M, Jütler B, Gonzalez-Vega L, Schicho J. Parameterizing surfaces with certain special support functions, including offsets of quadrics and rationally supported surfaces. J Symb Comput 2009;44:180–91.
[22] Sampoli M, Peternell M, Jüttler B. Exact parameterization of convolution surfaces and rational surfaces with linear normals. Comput Aided Geom Design 2006;23:179–92.
[23] Farin G. Curves and Surfaces for CAGD. San Francisco: Morgan-Kaufmann; 2002.
[24] Ahn YJ, Kim HO. Curvatures of the quadratic rational Bézier curves. Comput Math Appl 1998;36:71–83.
[25] Bartoň M, Hanniel I, Elber G, Kim M-S. Precise Hausdorff distance computation between polygonal meshes. Comput Aided Geom Design 2010;27:580–91.
[26] Emery JD. The definition and computation of a metric on plane curves. Comput Aided Design 1986;18:25–8.
[27] Elber G, Lee IK, Kim M-S. Comparing offset curve approximation method. IEEE Comput Graph Appl 1997;17(3):62–71.
[28] Hur S, Kim T. Finding the best conic approximation to the convolution curve of two compatible conics based on Hausdorff distance. Comput Aided Design 2009;41:513–24.
[29] Lee IK, Kim M-S, Elber G. Polynomial/rational approximation of Minkowski sum boundary curves. Graph Models Image Process 1998;60:136–65.
[30] Peternell M, Odehnal B. Convolution surfaces of quadratic triangular Bézier surfaces. Comput Aided Geom Design 2008;25:116–29.
[31] Kim YS. Bézier approximation of offset curves and Quadratic interpolation of plane curves. Ph.D. thesis. Ajou University; 2004.